Luminescent Silver(I) and Copper(I) Systems Containing Pyridyl Phosphine Bridges

Olga Crespo, M. Concepción Gimeno, Antonio Laguna, and Carmen Larraz

Departamento de Química Inorgánica, Instituto de Ciencia de Materiales de Aragón,
Universidad de Zaragoza-CSIC E-50009 Zaragoza, Spain

Reprint requests to Prof. M. C. Gimeno. E-mail: gimeno@unizar.es

Z. Naturforsch. **2009**, *64b,* 1525 – 1534; received September 29, 2009

Dedicated to Professor Hubert Schmidbaur on the occasion of his 75th birthday

Luminescent silver(I) and copper(I) complexes containing pyridylphosphine ligands have been synthesized and structurally characterized by single crystal X-ray diffraction methods. The reaction of Ag(OTf) (OTf = trifluoromethanesulfonate) with 2-pyridyldiphenylphosphine in different molar ratios gives the species $[Ag_2(OTf)_2(\mu\text{-}PPh_2py)_2]$ (**1**), $[Ag(PPh_2py)_2]OTf$ (**2**), $[Ag(PPh_2py)_3]OTf$ (**3**), and $[Ag_2(PPh_2py)_3](OTf)_2$ (**4**) with several modes of coordination of the pyridylphosphine. The oxidation of the phosphine in compound **4** gave $[Ag_2(OTf)(\mu\text{-}PPh_2py)_2(OPPh_2py)]OTf$ (**5**) which has been structurally characterized. It shows two bridging phosphine ligands and one chelating $OPPh_2py$ ligand. The reactions of the silver salt with bis(2-pyridyl)phenylphosphine in different molar ratios affords the complex $[Ag_2(OTf)_2(\mu\text{-}PPhpy_2)_2]$ (**6**), while the corresponding reactions with $[Cu(NCMe)_4]PF_6$ lead to two different compounds, namely $[Cu_2(NCMe)_2(\mu\text{-}PPhpy_2)_2](PF_6)_2$ (**7**) and $[Cu_2(PPhpy_2)_2(\mu\text{-}PPhpy_2)_2](PF_6)_2$ (**8**). All complexes exhibit luminescence in the solid state at room temperature and at 77 K.

Key words: Silver, Copper, Pyridylphosphines, Luminescence, Metallophilic Interactions

Introduction

Luminescent d^{10} compounds [1, 2] have received increasing attention over the past decade because of their interesting photophysical and photochemical properties, their possible applications in OLED display technology [3, 4], as dopant emitters [5 – 9] and in sensor development for luminescence-based detection of volatile organic compounds (VOCs) [10 – 14]. For such applications, polynuclear d^{10} complexes that exhibit intense, long-living luminescence in the solid state at ambient temperatures with emission energies spanning the visible spectrum appear particularly attractive [1, 2]. In many of these compounds the interesting luminescent properties are enhanced in the presence of the metallophilic interactions [15, 16], and this is particularly true for gold complexes but also to a lesser extend for the silver and copper derivatives.

Bridging ligands play a key role in the formation and properties of polynuclear d^{10} complexes by helping to facilitate intramolecular metallophilic interactions. One notable ligand in this regard is 2-pyridyldiphenylphosphine (PPh_2py) [17, 18]. This unsymmetrical ligand, which forms a rigid bridge between two metal ions, was first used by Balch and coworkers for comparison with the symmetrical bridging ligand bis(diphenylphosphino)methane (dppm) and for the construction of heterobimetallic systems [19]. A similar ligand, which has been less explored in coordination chemistry, is the bis(2-pyridyl)phenylphosphine ($PPhpy_2$) which has an additional pyridine ring and thus can act as tridentate ligand.

Specific examples with two bridging ligands in group 11 metal complexes include the dimeric Au(I) complex $[Au_2(\mu\text{-}PMe_2py)_2](BF_4)_2$ with a remarkably short gold-gold distance [20], the dimeric Cu(I) complexes $[Cu_2(NCMe)_2(\mu\text{-}PPh_2py)_2](PF_6)_2$ and $[Cu_2(NCMe)(\mu\text{-}PPh_2py)_3](BF_4)_2$, [21], and the silver complexes $[Ag_2(NO_3)_2(\mu\text{-}PPh_2py)_2]$, $[Ag_4(NO_3)_2(\mu\text{-}NO_3)(\mu\text{-}PPh_2py)_4]^+$, $[Ag_2(\mu\text{-}PPh_2py)_2(PPh_2py)]^{2+}$, and $[Ag_2Cl_2(\mu\text{-}PPh_2py)(PPh_2py)_2]$ [22], and a variety of adducts of the type $[AgX(PPh_2py)]$ [23] (X = Cl, Br, NO_3, SCN, ClO_4, BF_4, O_2CCF_3). With the $PPhpy_2$ ligand the gold compound $[Au(C_6F_5)(PPhpy_2)]$ [24], the silver complex $[Ag_2(NCMe)_2(PPhpy_2)_2](ClO_4)_2$ [25], the copper complexes $[Cu_2Cl_2(\mu\text{-}PPhpy_2)_2]$

0932–0776 / 09 / 1100–1525 $ 06.00 © 2009 Verlag der Zeitschrift für Naturforschung, Tübingen · http://znaturforsch.com

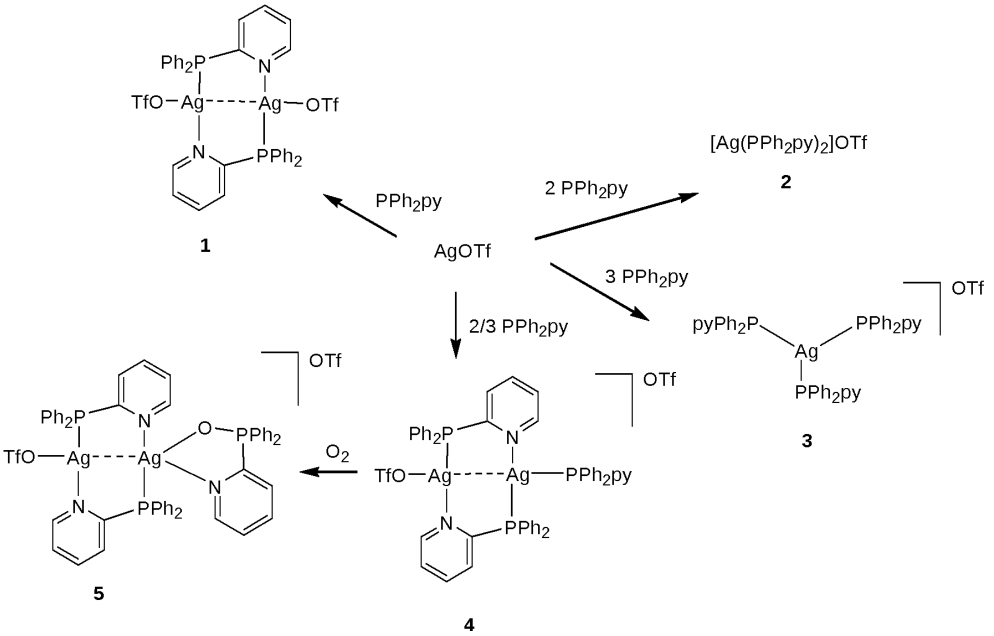

Scheme 1.

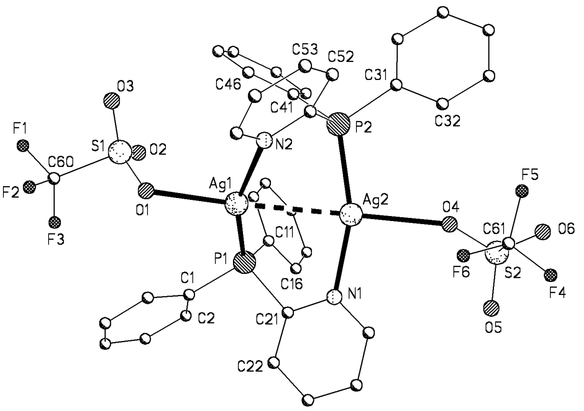

Fig. 1. Molecular structure of complex **1** in the crystal. Hydrogen atoms have been omitted for clarity. Radii are arbitrary.

[26] and $[Cu_2(NCMe)_2(\mu\text{-}PPhpy_2)_2](ClO_4)_2$ [27], and palladium-copper [28] derivatives have been described.

Here we report on the synthesis of silver(I) and copper(I) complexes with the PPh_2py and $PPhpy_2$ ligands. Depending on the molar ratio, several coordination types have been achieved, and in the dinuclear derivatives metallophilic bonding has been observed only for silver complexes. The luminescence behavior of these complexes has been studied. Regardless of the metal different emissions have been observed depending on the phosphine ligand. A mixed intraligand and LMCT (pyridine-to-metal) transitions are possible as the origin of these emissions.

Results and Discussion

We studied the reactions of silver trifluoromethanesulfonate with the 2-pyridyldiphenylphosphine ligand in several molar ratios in order to investigate the structures of these complexes and their luminescence properties. The reaction of Ag(OTf) with one equivalent of PPh_2py in acetone leads to the dinuclear derivative $[Ag_2(OTf)_2(\mu\text{-}PPh_2py)_2]$ (**1**) (see Scheme 1). The $^{31}P\{^1H\}$ NMR spectrum of **1** presents a broad temperature-dependent resonance, which is indicative of ligand exchange processes involving dissociation of the Ag–P bonds. At −90 °C a spectrum with 6 symmetric lines centered at 22.83 ppm occurs that is in agreement with bridging PPh_2py ligands; it corresponds to an AB system for the phosphorus atoms coupled to both silver nuclei with different coupling constants. Simulation of the spectrum agrees with the proposal.

The crystal structure determination of complex **1** shows the presence of a dinuclear bridging P,N unit forming an eight-membered ring where the silver atoms are also bonded to one oxygen atom of the triflate ligand. The molecule is shown in Fig. 1, and a selection of bond lengths and angles is given in Table 1. One of the silver atoms, Ag1, is also bonded to one oxygen atom of another triflate, O5,

Table 1. Selected bond lengths (Å) and angles (deg) for complex **1**[a].

Ag(1)–N(2)	2.259(3)	Ag(1)–Ag(2)	3.0438(5)
Ag(1)–P(1)	2.3707(9)	Ag(2)–N(1)	2.220(3)
Ag(1)–O(1)	2.433(2)	Ag(2)–P(2)	2.3816(9)
Ag(1)–O(5)$^{\#1}$	2.582(2)	Ag(2)–O(4)	2.570(2)
N(2)–Ag(1)–P(1)	156.61(7)	O(5)$^{\#1}$–Ag(1)–Ag(2)	97.38(5)
N(2)–Ag(1)–O(1)	87.95(9)	N(1)–Ag(2)–P(2)	160.92(7)
P(1)–Ag(1)–O(1)	115.41(6)	N(1)–Ag(2)–O(4)	95.73(9)
N(2)–Ag(1)–O(5)$^{\#1}$	79.48(8)	P(2)–Ag(2)–O(4)	103.29(6)
P(1)–Ag(1)–O(5)$^{\#1}$	106.29(6)	N(1)–Ag(2)–Ag(1)	85.79(7)
O(1)–Ag(1)–O(5)$^{\#1}$	75.53(8)	P(2)–Ag(2)–Ag(1)	75.46(2)
N(2)–Ag(1)–Ag(2)	83.12(7)	O(4)–Ag(2)–Ag(1)	164.65(5)
P(1)–Ag(1)–Ag(2)	73.72(2)		
O(1)–Ag(1)–Ag(2)	169.53(6)		

[a] Symmetry transformation used to generate equivalent atoms: $^{\#1}$ x, $-y+1/2$, $z+1/2$.

Table 2. Selected bond lengths (Å) and angles (deg) for complex **5**.

Ag(1)–N(1)	2.236(2)	Ag(2)–N(3)	2.282(2)
Ag(1)–P(1)	2.3857(6)	Ag(2)–N(2)	2.332(2)
Ag(1)–O(2)	2.5045(18)	Ag(2)–P(2)	2.3813(6)
Ag(1)–Ag(2)	3.0623(3)	Ag(2)–O(1)	2.5009(17)
N(1)–Ag(1)–P(1)	160.80(6)	N(3)–Ag(2)–O(1)	76.12(6)
N(1)–Ag(1)–O(2)	90.44(7)	N(2)–Ag(2)–O(1)	90.93(7)
P(1)–Ag(1)–O(2)	108.12(5)	P(2)–Ag(2)–O(1)	116.40(4)
N(1)–Ag(1)–Ag(2)	83.40(5)	N(3)–Ag(2)–Ag(1)	93.58(5)
P(1)–Ag(1)–Ag(2)	77.457(16)	N(2)–Ag(2)–Ag(1)	87.56(5)
O(2)–Ag(1)–Ag(2)	168.17(5)	P(2)–Ag(2)–Ag(1)	75.492(16)
N(3)–Ag(2)–N(2)	115.94(7)	O(1)–Ag(2)–Ag(1)	167.70(4)
N(3)–Ag(2)–P(2)	132.43(5)	P(3)–O(1)–Ag(2)	113.49(9)
N(2)–Ag(2)–P(2)	109.77(5)		

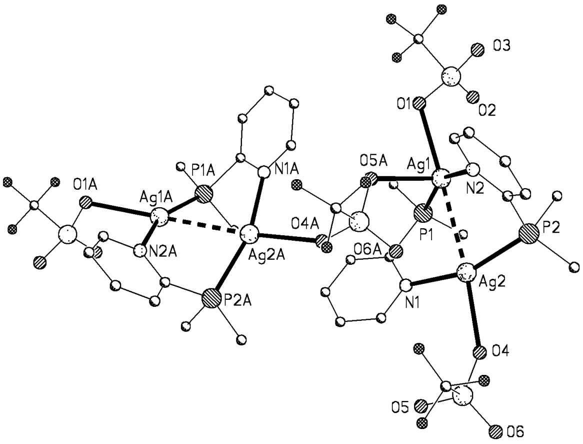

Fig. 2. One-dimensional zig-zag coordination polymer of complex **1** in the crystal.

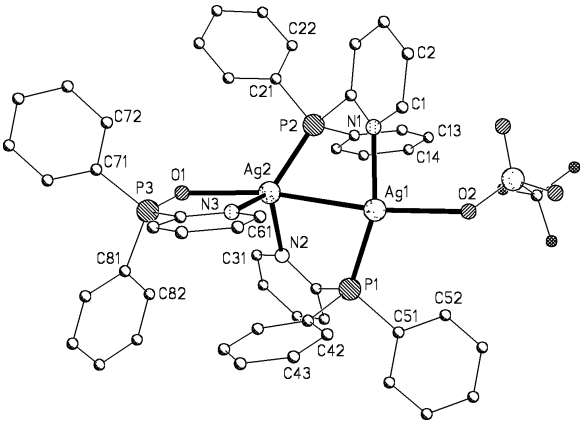

Fig. 3. Structure of the cation of complex **5** in the crystal. Hydrogen atoms have been omitted for clarity. Radii are arbitrary.

at a distance of 2.582(2) Å. The bridging nature of these triflate ligands leads to the formation of a one-dimensional zig-zag polymer (Fig. 2). The Ag–Ag distance of 3.044(1) Å is similar to others found in dinuclear complexes with bridging ligands such as $[Ag_2(\mu\text{-}PPh_2CH_2SPh)_2](ClO_4)_2$ (2.9501(8), 2.9732(9) Å) [29], with a P,S ligand, $[Ag_2(NO_3)_2\{\mu\text{-}PPh_2(Bzim)\}_2]$ (3.970 Å) [30], with a P,N ligand, and $[Ag_2(\mu\text{-}PP)_2]^{2+}$ (2.890–3.095 Å) (PP = diphosphine) in which the existence of argentophilic interactions was suggested based on spectroscopic evidence [31]. The geometry around the silver centers in **1** is very irregular. In both cases the angles N–Ag–P are very distorted from a linear geometry with angles N2–Ag1–P1 of 156.61(7) and N1–Ag2–P2 of 160.92(7)°. Consequently the other angles are also irregular, but Ag2 can be considered to be in a tetrahedral environment, whereas the geometry around Ag1 (bonded to two triflate ligands) can be regarded as trigonal pyramidal. The Ag–P and Ag–N distances are 2.3707(9), 2.3816(9) Å and 2.259(3), 2.220(3) Å, respectively, and are in the same range as those found in the $[Ag_2(NO_3)_2\{\mu\text{-}PPh_2(Bzim)\}_2]$ [30], which also contains a P,N bridging ligand. The Ag–O distances are very different, with 2.433(2) Å for the terminal triflate ligand and 2.582(2) and 2.570(2) Å for the bridging triflate.

The reaction of Ag(OTf) and PPh_2py in a molar ratio of 1:2 gives a complex of stoichiometry $[Ag(PPh_2py)_2]OTf$ (**2**). There are several possible modes of coordination of two phosphine ligands to the silver center: the complex can be mononuclear with two chelate pyridyl-phosphine ligands, dinuclear with two P,N-bridging ligands and one terminal P-ligand bonded to each silver center, or dinuclear with two bridging P,N- and two chelating P,N-ligands. Consequently, although the analytical data correspond to the

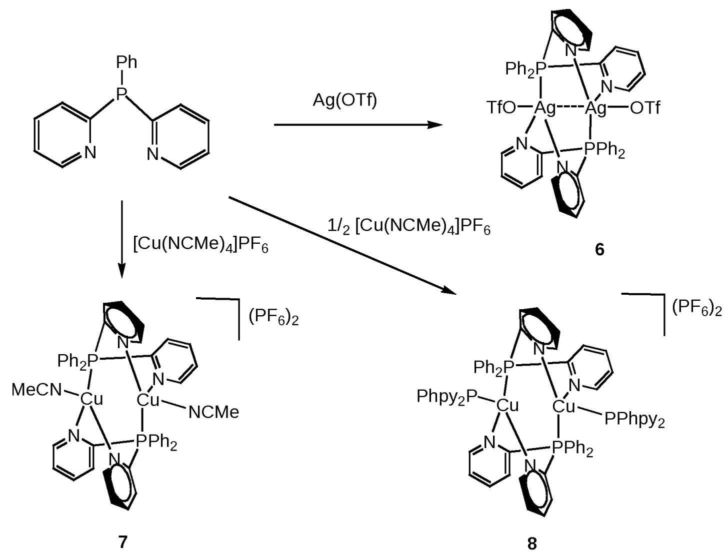

Scheme 2.

proposed stoichiometry, the NMR data at low temperature show the presence of several complexes that may corresponds to all the possible isomers.

Complexes [Ag(PPh$_2$py)$_3$]OTf (**3**) and [Ag$_2$(PPh$_2$py)$_3$](OTf)$_2$ (**4**) have also been prepared by treatment of AgOTf with the phosphine in molar ratios of 1:3 and 2:3. The proposed structures correspond to a trigonal-planar geometry for complex **3** and a dinuclear compound with bridging P,N ligands and a terminal phosphine ligand for complex **4**, similar to the structure obtained for the perchlorate salt (Scheme 1). The NMR data also agree with those of the perchlorate salt [22c]. During crystallization of compound **4** crystals of the oxidized product [Ag$_2$(μ-PPh$_2$py)$_2$(OPPh$_2$py)](OTf)$_2$ (**5**) were obtained. Its molecular structure is shown in Fig. 3, and a selection of bond lengths and angles are given in Table 2. The complex consists of a dinuclear unit with two bridging P,N ligands in which one of the silver atoms is bonded to a chelating N,O-ligand and the other one to the oxygen atoms of the triflate unit. There is a short Ag$\cdots$Ag distance of 3.023(3) Å which is similar to that found in complex **1**. The geometry around the silver center Ag2 is strongly distorted tetrahedral with an angle P2–Ag2–N2 of 132.43(5)°, and Ag1 shows a very irregular trigonal-planar geometry with a wide N1–Ag1–P1 angle of 160.80(6)°. Ag1 displays a long intermolecular contact of 2.689 Å to one oxygen atom of the triflate ligand leading to dimeric units, as shown in Fig. 4. The Ag–N and Ag–P distances are also very similar to those in compound **1**.

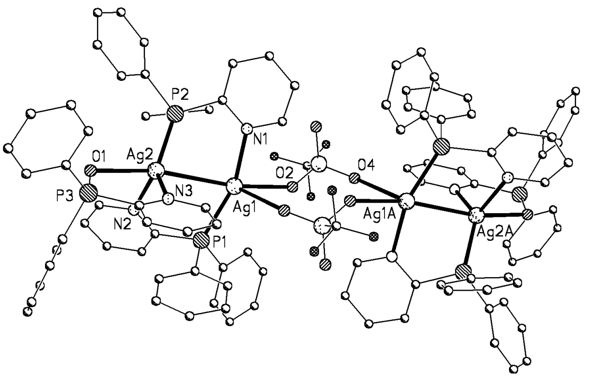

Fig. 4. Association into dimers of complex **5**.

The reactivity of the bis(2-pyridyl)phenylphosphine ligand towards silver(I) and copper(I) has also been studied. Treatment of PPhpy$_2$ with Ag(OTf) leads to the formation of the dinuclear species [Ag$_2$(OTf)$_2$(μ-PPh$_2$py)$_2$] (**6**) independently from the molar ratios used (1:1 or 2:1, see Scheme 2). The ^{1}H NMR spectrum shows the resonances of the pyridine and phenyl rings of the phosphines, and the ^{31}P{^{1}H} NMR spectrum displays a broad resonance at 22.0 ppm that splits into two broad doublets at low temperature. The ((+)-LSI) mass spectrum shows the cation molecular peak at *m/z* = 893 ([Ag$_2$(OTf)(PPhpy$_2$)$_4$]$^+$, 15 %), and the most intense peak appears at *m/z* = 371 ([Ag(PPhpy$_2$)]$^+$, 100 %).

The structure of complex **6** has been established by X-ray diffraction, and the molecule is shown in Fig. 5. A selection of bond lengths and angles is collected in

Table 3. Selected bond lengths (Å) and angles (deg) for complex **6**[a].

Ag(1)–N(1)$^{\#1}$	2.339(4)	Ag(1)–O(1)	2.497(4)
Ag(1)–N(2)$^{\#1}$	2.352(5)	Ag(1)–Ag(1)$^{\#1}$	3.1953(9)
Ag(1)–P(1)	2.3727(16)		
N(1)$^{\#1}$-Ag(1)-N(2)$^{\#1}$	82.53(15)	P(1)-Ag(1)-O(1)	109.49(16)
N(1)$^{\#1}$-Ag(1)-P(1)	134.85(13)	N(1)$^{\#1}$-Ag(1)-Ag(1)$^{\#1}$	84.97(11)
N(2)$^{\#1}$-Ag(1)-P(1)	128.60(10)	N(2)$^{\#1}$-Ag(1)-Ag(1)$^{\#1}$	81.40(9)
N(1)$^{\#1}$-Ag(1)-O(1)	84.08(15)	P(1)-Ag(1)-Ag(1)$^{\#1}$	71.33(3)
N(2)$^{\#1}$-Ag(1)-O(1)	107.99(19)	O(1)-Ag(1)-Ag(1)$^{\#1}$	164.47(12)

[a] Symmetry transformation used to generate equivalent atoms: $^{\#1}$ $-x+2$, $-y+2$, $-z$.

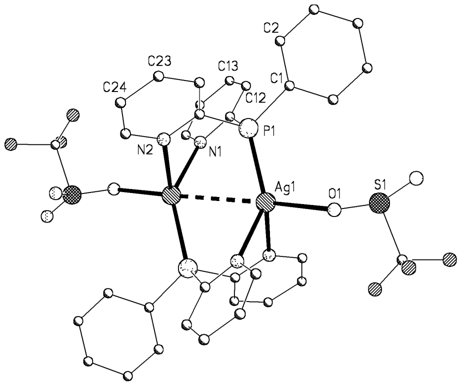

Fig. 5. Molecular structure of complex **6** in the crystal. Hydrogen atoms have been omitted for clarity. Radii are arbitrary.

Table 3. The complex crystallizes as a dimer with a short Ag(I)···Ag(I) contact of 3.1953(9) Å, slightly longer than that of the corresponding PPh_2py derivative. Contrary to the situation in complex **1** the triflate units in **6** are acting as monodentate ligands, and the geometry for both silver(I) atoms is distorted tetrahedral (not taking into account the argentophilic interaction) with a narrow N–Ag–N angle of 82.53(15)° and a very regular P–Ag–O angle of 109.49(16)°. The Ag–N distances are 2.339(4) and 2.352(5) Å, and the Ag–P bond length is 2.3727(16) Å which is in same range as those found in the acetonitrile derivative $[Ag_2(NCMe)_2(\mu\text{-}PPhpy_2)_2](ClO_4)_2$ [25].

The corresponding reactions of bis(2-pyridyl)phenylphosphine with $[Cu(NCMe)_4]PF_6$, in a 1:1 or 2:1 molar ratio, lead to two different compounds, namely $[Cu_2(NCMe)_2(\mu\text{-}PPhpy_2)_2](PF_6)_2$ (**7**) and $[Cu_2(PPhpy_2)_2(\mu\text{-}PPhpy_2)_2](PF_6)_2$ (**8**) (Scheme 2). The $^{31}P\{^1H\}$ NMR spectra show a singlet for complex **7** at −6.36 ppm, indicating the equivalence of the phosphorus atoms, whereas for compound **8** a very broad resonance is observed at 3.2 ppm even at low temperature, probably arising from a rapid exchange be-

Table 4. Selected bond lengths (Å) and angles (deg) for complex **7**[a].

Cu(1)–N(3)	2.032(3)	Cu(1)–P(1)	2.1940(11)
Cu(1)–N(2)$^{\#1}$	2.062(3)	Cu(1)–Cu(1)$^{\#1}$	3.5303(10)
Cu(1)–N(1)$^{\#1}$	2.067(3)		
N(3)-Cu(1)-N(2)$^{\#1}$	99.06(12)	N(3)-Cu(1)-P(1)	116.38(9)
N(3)-Cu(1)-N(1)$^{\#1}$	100.68(12)	N(2)$^{\#1}$-Cu(1)-P(1)	122.47(8)
N(2)$^{\#1}$-Cu(1)-N(1)$^{\#1}$	92.33(11)	N(1)$^{\#1}$-Cu(1)-P(1)	120.87(8)

[a] Symmetry transformation used to generate equivalent atoms: $^{\#1}$ $-x+1$, $-y$, $-z+1$.

Table 5. Selected bond lengths (Å) and angles (deg) for complex **8**[a].

Cu(1)–N(1)$^{\#1}$	2.043(3)	Cu(1)–P(1)	2.2385(14)
Cu(1)–N(2)$^{\#1}$	2.064(3)	Cu(1)–P(2)	2.2485(11)
N(1)$^{\#1}$-Cu(1)-N(2)$^{\#1}$	101.96(13)	N(1)$^{\#1}$-Cu(1)-P(2)	110.44(10)
N(1)$^{\#1}$-Cu(1)-P(1)	108.01(10)	N(2)$^{\#1}$-Cu(1)-P(2)	103.30(9)
N(2)$^{\#1}$-Cu(1)-P(1)	105.91(10)	P(1)-Cu(1)-P(2)	124.67(4)

[a] Symmetry transformation used to generate equivalent atoms: $^{\#1}$ $-x$, $-y+1$, $-z$.

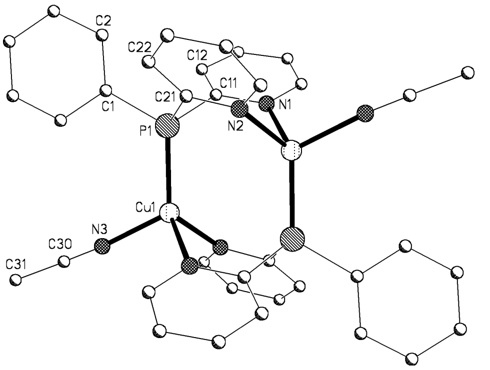

Fig. 6. Structure of the cation of complex **7** in the crystal. Hydrogen atoms have been omitted for clarity. Radii are arbitrary.

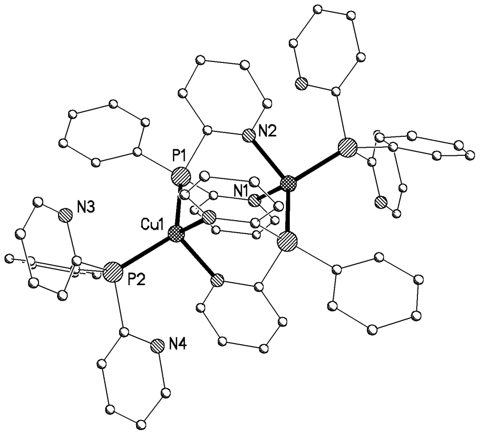

Fig. 7. Structure of the cation of complex **8** in the crystal. Hydrogen atoms have been omitted for clarity. Radii are arbitrary.

Table 6. DRUV and Luminescence studies.

Compound	RDUV	$\lambda_{\text{emis}}{}^{a}$ (λ_{ex})^{b} 298 K	$\lambda_{\text{emis}}{}^{a}$ (λ_{ex})^{b} 77 K	τ (μs) 298 K
$[Ag_2(OTf)_2(\mu\text{-}PPh_2py)_2]$ (**1**)	310–360 450	497 (407)	479 (360)	53.7
$[Ag(PPh_2py)_2]OTf$ (**2**)	310–360	491 (366)	455(325)	51.8
$[Ag(PPh_2py)_3]OTf$ (**3**)	240 290–400	494 (407)	436 (322) 497 (407)	25.7
$[Ag_2(PPh_2py)_3](OTf)_2$ (**4**)	240 300–400	496 (400)	482 (400) 464 (310)	10.2
$[Ag_2(OTf)_2(\mu\text{-}PPhpy_2)_2]$ (**6**)	220 300–250 360–400	547 (388)	450 (308) 555 (360)	62
$[Cu_2(NCMe)_2(\mu\text{-}PPhpy_2)_2](PF_6)_2$ (**7**)	210 300–350 360–400	543 (360)	514 (319)	13
$[Cu_2(PPhpy_2)_2(\mu\text{-}PPhpy_2)_2](PF_6)_2$ (**8**)	260 340–450	550 (380)	510 (315) 568 (360)	18

[a] Emission maxima in nm; [b] excitation maxima in nm.

tween the phosphine sites on the NMR time scale. The mass spectra for both complexes show similar peaks with similar abundances arising from the fragments $[Cu(PPhpy_2)]^+$ at *m/z* = 327 (100 %), $[Ag(PPhpy_2)_2]^+$ at *m/z* = 591 (16 %) and $[Ag_2(PPhpy_2)_2]^{2+}$ at *m/z* = 654 (6 %).

The crystal structures of complexes **7** and **8** have been determined, and the cations are shown in Figs. 6 and 7, respectively. A selection of bond lengths and angles are collected in Tables 4 and 5. The structure of complex **7** is similar to that recently communicated with the perchlorate anion [27] and consists of two copper atoms bridged by two $PPhpy_2$ ligands and additionally bonded to an acetonitrile molecule. The coordination around the copper atoms is distorted tetrahedral, and the distance Cu···Cu is 3.5303(10) Å, which can be considered as a weak copper-copper bonding interaction. The structure of complex **8** is similar, but now the acetonitrile positions are occupied by a terminal phosphine ligand bonded *via* the phosphorus atoms. The Au–N distances are very similar, 2.043(3) and 2.064(3) Å, whereas the Ag–P bond lengths are slightly different, 2.2385(14) and 2.2485(11) Å, the shortest corresponding to the bridging phosphine ligand.

Luminescence studies

The diffuse reflectance ultraviolet visible spectra (DRUV) were recorded for all the complexes. The spectra of **3**, **4**, **6**–**8** consist of one band with maxima between 220 and 260 nm, depending on the complex, and one or two additional bands in the 300–450 nm region (Table 6). Absorptions at higher energies than 310 nm are not observed in **1** and **2**.

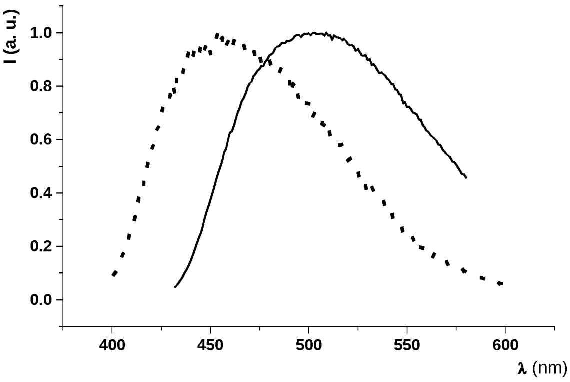

Fig. 8. Emission spectra of complexes **2** (straight line) and **7** (dashed line).

All the complexes are emissive in the solid state, both at r. t. and at 77 K. They display one or two emissions (Table 6) in the range from 436 to 568 nm. Lifetimes measured at r. t. are in the microsecond range, which points to a phosphorescence nature of the emissions. The general trend is that the emission maxima for complexes with the phosphine $PPhpy_2$ appear at lower energies than those containing PPh_2py (Fig. 8 illustrates this behavior for complexes **2** and **7**), although the metal (copper or silver) is another factor to be taken into account. The emissions observed for complexes **1**–**4** (which contain PPh_2py) resemble in general the energies of the free monophosphine and are probably due to intraligand (IL, PPh_2py) [32] transitions modified through the coordination to silver. Furthermore compounds **3** and **4** display two bands at 77 K. Thus, a contribution of pyridine-to-silver charge-transfer transitions to the emissive behavior of this complex can be postulated.

Complexes **6**–**8** (which contain $PPhpy_2$) display emissions at higher energies than **1**–**4**. The luminescence of $[Cu_2(NCMe)_2(\mu\text{-}PPhpy_2)_2]SO_4$ and polymeric $[Cu_2(\mu\text{-}PPhpy_2)_2(\mu\text{-}SO_4)]_\infty$ has been studied in the solid state at r. t. Both complexes display green emission [27] which is consistent with our results obtained for **7**. It is interesting to compare the emission of $[Cu_2(NCMe)_2(\mu\text{-}PPhpy_2)_2](PF_6)_2$ (**7**), $[Cu_2(NCMe)_2(\mu\text{-}PPhpy_2)_2]SO_4$ and $[Cu_2(\mu\text{-}PPhpy_2)_2(\mu\text{-}SO_4)]_\infty$ with that of the analogous silver complexes $[Ag_2(NCMe)_2(\mu\text{-}PPhpy_2)_2](ClO_4)_2$ and $[Ag_2(\mu\text{-}PPhpy_2)_2\{1,3,5\text{-}C_6H_3(CO_2)_2(CO_2H)\}]_\infty$ [25]. The blue emission of the silver complexes around 440 nm indicates that metal-metal interactions and the axial ligand do not have an important effect on the energy of the emission which was postulated to originate from intra-ligand transitions and resembles those observed at 77 K for $[Ag_2(OTf)_2(\mu\text{-}PPhpy_2)_2]$ (**6**). Intra-ligand ($PPhpy_2$) transitions [27], modified by the presence of copper and silver, could thus be responsible for the luminescence of **6**–**8**, but such an origin would not explain the different emissions of the analogous complexes $[Ag_2(NCMe)_2(\mu\text{-}PPhpy_2)_2](ClO_4)_2$, (blue emissive) [27] and $[Cu_2(NCMe)_2(\mu\text{-}PPhpy_2)_2]SO_4$ or $[Cu_2(NCMe)_2(\mu\text{-}PPhpy_2)_2](PF_6)_2$ (**7**) (green emissive) [25]. Pyridine-to-ligand charge transfer transitions (LMCT, py → Cu or Ag) could be responsible for this luminescence, however, since a similar red shift when going from silver to copper has been described for acetylide complexes [33], although the emission of $[Ag_2(OTf)_2(\mu\text{-}PPhpy_2)_2]$ (**6**) does not follow this pattern. Two bands are observed for **6** and **8** at 77 K indicating that the situation may be more complicated. Thus, the origin of the emissions probably is mixed IL and LMCT (py → Cu or Ag), but predominantly LMCT.

Conclusions

Silver(I) complexes with the ligand 2-pyridyldiphenylphosphine have been synthesized and present several modes of coordination of the pyridylphosphine. The oxidation of $[Ag_2(PPh_2py)_3](OTf)_2$ (**4**) gave $[Ag_2(OTf)(\mu\text{-}PPh_2py)_2(OPPh_2py)]OTf$, which has been structurally characterized. The silver(I) and copper(I) complexes with the bis(2-pyridyl)phenylphosphine ligand are dinuclear species with a tridentate P,N,N phosphine and an equatorial ligand that can be triflate for silver and acetonitrile or another phosphine ligand for copper. Metallophilic interactions are only present for the silver derivatives. The complexes are emissive in the solid state, both at 298 and 77 K. The emission maxima appear at lower energies for complexes with the $PPhpy_2$ ligand. The origin of the emission is postulated as mixed IL (monophosphine) and LMCT (py → Cu or Ag), although IL transitions probably dominate in complexes containing PPh_2py, and LMCT are postulated as more important for the luminescence of the compounds containing $PPhpy_2$.

Experimental Section

General procedure

Infrared spectra were recorded in the range of 4000–200 cm^{-1} on a Perkin-Elmer 883 spectrophotometer using Nujol mulls between polyethylene sheets. C, H, N and S analyses were carried out with a Perkin-Elmer 2400 microanalyzer. Mass spectra were recorded on a VG Autospec instrument, with the liquid secondary-ion mass spectrometry (MS ((+)-LSI)) technique, using nitrobenzyl alcohol as matrix. NMR spectra were recorded on Varian Unity 300 and Bruker ARX 300 spectrometers in $CDCl_3$. Chemical shifts are cited relative to $SiMe_4$ (^1H, external), 85 % H_3PO_4 (^{31}P, external), or $CFCl_3$ (^{19}F, external). The starting materials $PPhpy_2$ [34] and $[Cu(NCMe)_4]PF_6$ [35] were prepared by published procedures. Other compounds were commercially available. DRUV spectra were recorded with a UnicamUV-4 spectrophotometer equipped with a Spectralon RSA-UC-40 Labsphere integrating sphere. The solid samples were mixed with dried KBr and placed in a home-made cell equipped with a quartz window. The intensities were recorded in Kubelka-Munk units. Steady-state photoluminescence spectra were recorded with a Jobin-Yvon Horiba Fluorolog FL-3-11 spectrometer using band pathways of 3 nm for both excitation and emission. Phosphorescence lifetimes were recorded with a Fluoromax phosphorimeter accessory containing a UV xenon flash tube at a flash rate between 0.05 and 25 Hz. The lifetime data were fit using the Jobin-Yvon software package DATAMAX 2.20 [36] and the ORIGIN 5.0 program [37].

Preparations

*Synthesis of $[Ag_2(OTf)_2(\mu\text{-}PPh_2py)_2]$ (**1**)*

To a solution of Ag(OTf) (0.026 g, 0.1 mmol) in 20 mL of acetone was added PPh_2py (0.026 g, 0.1 mmol) and the solution stirred for 30 min. Evaporation of the solvent to *ca.* 2 mL

Table 7. Crystal structure data for complexes **1**, **5**, **6**, **7**, and **8**.

Compound	**1**	**5**	**6**	**7**	**8**
Formula	$C_{36}H_{26}Ag_2F_6N_2O_6P_2S_2$	$C_{57}H_{52}Ag_2F_6N_3O_8P_3S_2$	$C_{17}H_{13}AgF_3N_2O_3PS$	$C_{40}H_{38}Cu_2F_{12}N_8P_4$	$C_{34}H_{30}Cl_2CuF_6N_4P_3$
M_r	1040.40	1393.79	521.19	1109.76	835.97
Habit	pale-yellow prism	pale-yellow prism	pale-yellow plate	colorless needle	colorless prism
Crystal size, mm^3	0.28 × 0.20 × 0.16	0.24 × 0.20 × 0.16	0.22 × 0.16 × 0.10	0.22 × 0.07 × 0.07	0.25 × 0.20 × 0.18
Crystal system	monoclinic	triclinic	monoclinic	monoclinic	triclinic
Space group	$P2_1/c$	$P\bar{1}$	$P2_1/n$	$P2_1/c$	$P\bar{1}$
a, Å	12.400(2)	13.5195(7)	12.733(3)	8.9781(18)	10.154(2)
b, Å	27.660(5)	14.6439(7)	9.923(2)	28.264(6)	13.549(3)
c, Å	11.555(2)	15.6835(8)	15.140(3)	9.1630(18)	14.963(3)
α, deg	90	99.4870(10)	90	90	67.06(3)
β, deg	109.462(3)	107.1560(10)	98.84(3)	92.92(3)	79.20(3)
γ, deg	90	100.6360(10)	90	90	75.34(3)
V, Å^3	3736.6(11)	2835.3(2)	1890.3(7)	2322.2(8)	1825.1(6)
Z	4	2	4	2	2
D_X, g cm^{-3}	1.85	1.63	1.83	1.58	1.52
μ, mm^{-1}	1.3	0.9	1.3	1.1	0.9
$F(000)$, e	2064	1408	1032	1120	848
T, °C	−173	−173	−173	−173	−173
$2\theta_{max}$, deg	51	56.6	50	51	50
Refl. measured	21017	26925	11081	15474	11679
Refl. independent	6923	13207	3292	4287	6269
R_{int}	0.037	0.017	0.029	0.032	0.021
Min. / max. transm.	0.78 / 0.816	0.808 / 0.866	0.761 / 0.880	0.487 / 0.924	0.799 / 0.849
Parameters	505	717	271	451	451
wR (F^2, all refl.)	0.080	0.092	0.105	0.123	0.162
R [$I \geq 2\sigma(I)$]	0.033	0.033	0.048	0.052	0.058
S	1.091	1.032	1.108	1.084	1.076
$\Delta\rho_{max}$, e Å^{-3}	1.26	1.71	0.79	1.26	1.79

and addition of diethyl ether gave complex **1** as a white solid (0.050 g, 97 %). Calcd. (found) for $C_{18}H_{14}AgF_3NO_3PS$ (520.21): C 41.55 (41.31), H 2.71 (2.37), N 2.69 (2.45), S 6.16 (5.96). – ^{1}H NMR ($(CD_3)_2CO$): δ = 7.2 – 7.5 (m, 40H, Ph), 7.11 (d, 4H, py, J(HH) = 8.0 Hz), 7.58 (m, 4H, py), 7.84 (t, 4H, py, J(HH) = 8.0 Hz), 9.21 (m, 4H, py). – ^{31}P{^{1}H} NMR ($(CD_3)_2CO$, 183 K), $\delta_A \approx \delta_B$ = 22.83 (AB system, 2P, PPh_2py, $J(Ag^{109}P)$ = 767.1, $J(Ag^{107}P)$ = 673, $J(Ag^{109}P)$ = 673, $J(Ag^{107}P)$ = 590.1 Hz).

*Synthesis of [Ag(PPh$_2$py)$_2$]OTf (**2**)*

To a solution of Ag(OTf) (0.026 g, 0.1 mmol) in 20 mL of acetone was added PPh_2py (0.053 g, 0.2 mmol) and the solution stirred for 30 min. Evaporation of the solvent to *ca.* 2 mL and addition of diethyl ether gave complex **2** as a white solid (0.072 g, 93 %). Calcd. (found) for $C_{18}H_{14}AgF_3NO_3PS$ (783.48): C 53.65 (53.34), H 3.60 (3.18), N 3.57 (3.58), S 4.09 (3.99). – ^{1}H NMR ($(CD_3)_2CO$): δ = 7.2 – 7.55 (m, 20 + 2H, Ph + py), 7.61 (m, 2H, py), 7.94 (m, 2H, py), 8.96 (m, 2H, py). – ^{31}P{^{1}H} NMR ($CD_3)_2CO$): δ = 12.5 (s, br, 2P, PPh_2py).

*Synthesis of [Ag(PPh$_2$py)$_3$]OTf (**3**)*

To a solution of Ag(OTf) (0.026 g, 0.1 mmol) in 20 mL of acetone was added PPh_2py (0.079 g, 0.3 mmol) and the solution stirred for 30 min. Evaporation of the solvent to *ca.* 2 mL and addition of diethyl ether gave complex **3** as a white solid (0.091 g, 88 %). Calcd. (found) for $C_{52}H_{42}AgF_3N_3O_3P_3S$ (1046.76): C 59.66 (59.85), H 4.04 (4.38), N 4.01 (3.91), S 3.06 (3.59). – ^{1}H NMR ($(CD_3)_2CO$): δ = 7.26 – 7.36 (m, 30 + 3H, Ph + py), 7.11 (m, 3H, py), 7.69 (m, 3H, py), 8.45 (m, 3H, py). – ^{31}P{^{1}H} NMR ($(CD_3)_2CO$): δ = 7.4 (s, 3P, PPh_2py).

*Synthesis of [Ag$_2$(OTf)(PPh$_2$py)$_3$]OTf (**4**)*

To a solution of Ag(OTf) (0.052 g, 0.2 mmol) in 20 mL of acetone was added PPh_2py (0.079 g, 0.3 mmol) and the solution stirred for 30 min. Evaporation of the solvent to *ca.* 2 mL and addition of diethyl ether gave a white solid of complex **4** (0.106 g, 82 %). Calcd. (found) for $C_{53}H_{42}Ag_2F_6N_3O_6P_3S_2$ (1303.69): C 48.82 (48.56), H 3.24 (3.12), N 3.22 (3.04), S 4.91 (4.75). – ^{1}H NMR ($(CD_3)_2CO$): δ = 7.1 – 7.8 (m, 30 + 6H, Ph + py), 6.91 (m, 3H, py), 9.38 (m, 3H, py). – ^{31}P{^{1}H} NMR ($(CD_3)_2CO$): δ = 10.6 (t, br, 3P, PPh_2py).

*Synthesis of [Ag$_2$(OTf)$_2$(PPhpy$_2$)$_2$] (**6**)*

To a solution of Ag(OTf) (0.025 g, 0.1 mmol) in 20 mL of acetone was added $PPhpy_2$ (0.026 g, 0.1 mmol), and the mixture was stirred for 30 min. Evaporation of the solvent to *ca.* 5 mL and addition of *n*-hexane gave complex **6** as a white solid (0.09 g, 87 %). Calcd. (found) for $C_{34}H_{26}Ag_2F_6N_4O_6P_2S_2$ (1042.38): C 39.17 (39.34), H 2.51 (2.56), N 5.37 (5.34), S 6.15 (6.35). – MS ((+)-LSI): *m/z* (%) = 371 (100), $[Ag(PPhpy_2)]^+$). – ^{1}H NMR ($(CD_3)_2CO$): δ = 8.96 (d, 2H, py, ^3J(HH) = 4.7 Hz), 8.22 (t, 2H, py, ^3J(HH) = 7.8 Hz), 7.87 (d, br, 2H, py, ^3J(HH) $\sim$ 7.0 Hz), 7.82 – 7.63 (m, 5 + 2H, Ph). – $^{31}P\{^1H\}$ NMR ($(CD_3)_2CO$): δ = 22.07 (s, 2P, $PPhpy_2$); ($(CD_3)_2CO$, 183 K): δ = 22.41 (d, br, $PPhpy_2$, $J(AgP)_{av}$ = 428 Hz).

Synthesis of $[Cu_2(NCMe)_2(PPhpy_2)_2](PF_6)_2$ (7)

To a solution of $[Cu(NCMe)_4]PF_6$ (0.074 g, 0.2 mmol) in 20 mL of dichloromethane was added $PPhpy_2$ (0.052 g, 0.2 mmol) under argon atmosphere, and the mixture was stirred for 15 min, whereupon the solution turned yellow. Evaporation of the solvent to dryness and addition of *n*-hexane afforded complex **7** as a yellow solid (0.167 g, 75 %). Calcd. (found) for $C_{40}H_{44}Cu_2F_{12}N_8P_4$ (1115.79): C 43.29 (43.53), H 3.45 (3.31), N 10.09 (10.94). – ^{1}H NMR ($(CD_3)_2CO$): δ = 8.72 (d, 4H, py, ^3J(HH) = 4.6 Hz), 8.48 (dd, 4H, py, ^3J(HH) = 11.1, Hz, ^3J(HH) = 7.0 Hz), 8.01 – 7.42 (m, 10 + 8H, Ph + py), 3.75 (s, 6H, NCMe). – $^{31}P\{^1H\}$ NMR ($(CD_3)_2CO$): δ = −6.36, ($(CD_3)_2CO$, 183 K): δ = −3.09.

Synthesis of $[Cu_2(\mu\text{-}PPhpy_2)_2(PPhpy_2)_2](PF_6)_2$ (8)

To a solution of $[Cu(NCMe)_4]PF_6$ (0.074 g, 0.2 mmol) in 20 mL of dichloromethane $PPhpy_2$ (0.106 g, 0.4 mmol) was added under argon atmosphere, and the mixture was stirred for 15 min, whereupon the color turned yellow. Evaporation of the solvent to dryness and addition of *n*-hexane gave complex **8** as a yellow solid (0.212 g, 72 %). Calcd. (found) for $C_{64}H_{52}Cu_2F_{12}N_8P_6$ (1474.06): C 52.14 (52.31), H 3.55 (3.21), N 7.60 (7.49). – ^{1}H NMR ($(CD_3)_2CO$): δ = 9.00 – 6.8 (m, 20 + 32H, Ph + py). – $^{31}P\{^1H\}$ NMR $(CD_3)_2CO$), δ = 3.25, ($(CD_3)_2CO$, 183 K): δ = 4.44.

X-Ray structure determination

Data were measured using MoK_α radiation (λ = 0.71073 Å) on a Bruker SMART 1000 CCD (**1**, **5**) or a Xcalibur Oxford Diffraction diffractometer (**6**, **7**, **8**). Absorption corrections were based on multiple scans (program SADABS [38]). The structures were solved by Direct Methods, and refined by full-matrix least-squares on F^2 (SHELXL-97 [39]). All non-hydrogen atoms were refined anisotropically. H atoms were included using a riding model. Further details are given in Table 7.

CCDC 749320 – 749324 contain the supplementary crystallographic data for this paper. These data can be obtained free of charge from The Cambridge Crystallographic Data Centre *via* www.ccdc.cam.ac.uk/data_request/cif.

Acknowledgement

We thank the Ministerio de Ciencia e Innovación (CTQ2007-67273-C02-01) for financial support.

[1] S. Sibley, M. E. Thompson, P. E. Burrows, S. R. Forrest, in *Optoelectronic Properties of Inorganic Compounds*, (Eds.: D. M. Roundhill, J. P. Fackler, Jr.), Plenum Publishing Corp., New York, **1999**, pp. 29.

[2] a) V. W. W. Yam, K. K. W. Lo, *Chem. Soc. Rev.* **1999**, *28*, 323; b) W.-F. Fu, K.-C. Chan, K.-K. Cheung, C.-M. Che, *Chem. Eur. J.* **2001**, *7*, 4656; c) V. W. W. Yam, K. K. W. Lo, W. K. M. Fung, C. R. Wang, *Coord. Chem. Rev.* **1998**, *171*, 17; d) A. Vogler, H. Kunkely, *Coord. Chem. Rev.* **2001**, *219*, 489; e) P. C. Ford, E. Cariati, J. Bourassa, *Chem. Rev.* **1999**, *99*, 3625; f) C. H. Chen, J. Shi, *Coord. Chem. Rev.* **1998**, *171*, 161.

[3] M. A. Baldo, M. E. Thompson, S. R. Forrest, *Pure Appl. Chem.* **1999**, *71*, 2095.

[4] R. C. Evans, P. Douglas, C. J. Wiscom, *Coord. Chem. Rev.* **2006**, *250*, 2093.

[5] Q. Zhang, Q. Zhou, Y. Cheng, L. Wang, D. Ma, X. Jing, F. Wang, *Adv. Mater.* **2004**, *16*, 432.

[6] C. Fave, T.-Y. Cho, M. Hissler, C.-W. Chen, T.-Y. Luh, C.-C. Wu, R. Reau, *J. Am. Chem. Soc.* **2003**, *125*, 9254.

[7] Y. Ma, C.-M. Che, H.-Y. Chao, X. Zhou, W.-H. Chan, J. Shen, *Adv. Mater.* **1999**, *11*, 852.

[8] Y. Ma, X. Zhou, J. Shen, H.-Y. Chao, C.-M. Che, *Appl. Phys. Lett.* **1999**, *74*, 1361.

[9] Y.-G. Ma, W.-H. Chan, X.-M. Zhou, C.-M. Che, *New. J. Chem.* **1999**, *23*, 263.

[10] J. C. Vickery, M. M. Olmstead, E. Y. Fung, A. L. Balch, *Angew. Chem.* **1997**, *109*, 1227; *Angew. Chem., Int. Ed. Engl.* **1997**, *36*, 1179.

[11] M. A. Mansour, W. B. Connick, R. J. Lachicotte, H. J. Gysling, R. Eisenberg, *J. Am. Chem. Soc.* **1998**, *120*, 1329.

[12] E. J. Fernandez, J. M. López-de-Luzuriaga, M. Monge, M. E. Olmos, J. Perez, A. Laguna, A. A. Mohamed, J. P. Fackler, Jr., *J. Am. Chem. Soc.* **2003**, *125*, 2022.

[13] E. Y. Fung, M. M. Olmstead, J. C. Vickery, A. L. Balch, *Coord. Chem. Rev.* **1998**, *171*, 151.

[14] E. J. Fernández, J. M. López de Luzuriaga, M. Monge, M. E. Olmos, R. Puelles, A. Laguna, A. A. Mohamed, J. P. Fackler, Jr., *Inorg. Chem.* **2008**, *47*, 8069.

[15] a) P. Pyykkö, *Chem. Rev.* **1997**, *97*, 597; b) P. Pyykkö, *Angew. Chem.* **2004**, 116, 4512; *Angew. Chem. Int. Ed.* **2004**, *43*, 4412; c) P. Pyykkö, *Inorg. Chim. Acta* **2005**, *358*, 4113.

[16] H. Schmidbaur, *Gold Bull.* **2000**, *33*, 3.

[17] Z.-Z. Zhang, H. Cheng, *Coord. Chem. Rev.* **1996**, *147*, 1.

[18] G. R. Newkome, *Chem. Rev.* **1993**, *93*, 2067.

[19] a) J. P. Farr, M. P. Olmstead, A. L. Balch, *J. Am. Chem. Soc.* **1980**, *102*, 6654; b) A. Maisonnet, J. P. Farr, A. L. Balch, *Inorg. Chim. Acta* **1981**, *53*, L217; c) A. Maisonnet, J. P. Farr, M. P. Olmstead, C. T. Hunt, A. L. Balch, *Inorg. Chem.* **1982**, *21*, 3961; d) J. P. Farr, F. E. Wood, A. L. Balch, *Inorg. Chem.* **1983**, *22*, 3387; e) J. P. Farr, M. P. Olmstead, A. L. Balch, *Inorg. Chem.* **1983**, *22*, 1229; f) J. P. Farr, M. P. Olmstead, F. E. Wood, A. L. Balch, *J. Am. Chem. Soc.* **1983**, *105*, 792.

[20] Y. Inoguchi, B. Milewski-Mahria, H. Schmidbaur, *Chem. Ber.* **1982**, *115*, 3085.

[21] a) M. Maekawa, M. Munakata, S. Kitagawa, T. Yonezawa, *Bull. Chem. Soc. Jpn* **1991**, *64*, 2286; b) E. Lastra, M. P. Gamasa, J. Gimeno, M. Lanfranchi, A. Tiripicchio, *J. Chem. Soc., Dalton Trans.* **1989**, *8*, 1499.

[22] a) H. Liu, W. Liu, P. Zhang, M. Huang, L. S. Zheng, *J. Xi. Uni. Nat. Sci.* **1992**, *31*, 57; b) W. Liu, H. Liu, L. Zhang, D. Wu, H. Zhuang, *J. Xi. Uni. Nat. Sci.* **1995**, *34*, 946; c) A. Del Zotto, E. Zangrando, *Inorg. Chim. Acta* **1998**, *277*, 111; d) N. W. Alcock, P. Moore, P. A. Lampe, K. F. Mol, *J. Chem. Soc., Dalton Trans.* **1982**, 207.

[23] A. Congolani, Effendy, D. Martini, C. Pettinari, B. W. Skelton, A. H. White, *Inorg. Chim. Acta* **2006**, *359*, 2183.

[24] J. A. Casares, P. Espinet, J. M. Martín-Álvarez, V. Santos, *Inorg. Chem.* **2006**, *45*, 6628.

[25] T. Zhang, C. Ji, K. Wang, D. Hu, X. Meng, C. Chen, *Inorg. Chim. Acta* **2007**, *360*, 1609.

[26] T. Zhang, K. Wang, S. W. Ng, *Acta Crystallogr.* **2006**, *E62*, m3494.

[27] T. Zhang, C. Chen, Y. Qin, X. Meng, *Inorg. Chem. Commun.* **2006**, *9*, 72.

[28] T. Zhang, Y. Qin, D. Wu, C. Wang, C. Liu, *J. Coord. Chem.* **2005**, *58*, 1485.

[29] E. J. Fernández, J. M. López-de-Luzuriaga, M. Monge, M. A. Rodríguez, O. Crespo, M. C. Gimeno, A. Laguna, P. G. Jones, *Inorg. Chem.* **1998**, *37*, 6002.

[30] F. Bachechi, A. Burini, R. Galassi, A. Machioni, B. R. Pietroni, F. Ziarelli, C. Zuccaccia, *J. Organomet. Chem.* **2000**, *593*, 392.

[31] C.-M. Che, M. C. Tse, M. C. W. Chan, K. K. Cheung, D. L. Phillips, K. H. Leung, *J. Am. Chem. Soc.* **2000**, *122*, 2464.

[32] L. J. Hao, M. A. Manosur, R. J. Lachicotte, H. J. Gyslyng, R. Eisenberg, *Inorg. Chem.* **2000**, *39*, 5520.

[33] V. V. W. Yam, S. W. K. Choi, C. L. Chan, K. K. Cheung, *Chem. Commun.* **1996**, 2067.

[34] a) G. R. Newkome, D. C. Hager, *J. Org. Chem.* **1978**, *43*, 947; b) Y. Xie, C. Lee, Y. Yang, S. J. Rettig, B. R. James, *Can. J. Chem.* **1992**, *70*, 751; c) T. Zhang, Y. Qin, D. Wu, C. Wang, C. Liu, *J. Coord. Chem.* **2005**, *58*, 1485.

[35] G. J. Kubas, *Inorg. Synth.* **1979**, *19*, 90.

[36] DATAMAX 2.20. Jobin Yvon, Inc., Edison, N. J. (USA), **2001**.

[37] ORIGIN 5.0, Microcal Software, Inc., Northampton, M. A. (USA) **1991**.

[38] G. M. Sheldrick, SADABS (version 2.03), Program for Empirical Absorption Correction of Area Detector Data, University of Göttingen, Göttingen (Germany) **2002**.

[39] G. M. Sheldrick, SHELXL-97, Program for the Refinement of Crystal Structures, University of Göttingen, Göttingen (Germany) **1997**. See also: G. M. Sheldrick, *Acta Crystallogr.* **2008**, *A64*, 112.